International Conference on Ships and Offshore Structures
ICSOS 2017
11 – 13 September 2017, Shenzhen, China

A life-cycle cost model for the reliability-based design of disconnectable FPSO mooring lines

José Manuel Cabrera-Miranda[a,b], Patrícia Mika Sakugawa[c], Rafael Corona-Tapia[d], Jeom Kee Paik[a,b,e,*]

[a]*Department of Naval Architecture and Ocean Engineering, Pusan National University, Busan 46241, Republic of Korea*
[b]*The Korea Ship and Offshore Research Institute (The Lloyd's Register Foundation Research Centre of Excellence), Pusan National University, Busan 46241, Republic of Korea*
[c]*Department of Mechanical Engineering & Post-Graduate Program in Science and Petroleum Engineering, University of Campinas, Campinas, São Paulo, Brazil*
[d]*Infraestructura y Evaluación, Coordinación de Diseño, Gerencia de Administración de Asignaciones en Aguas Profundas, Bloques Norte, Pemex Exploración y Producción, Tampico 89000, Tamaulipas, México*
[e]*Department of Mechanical Engineering, University College London, London WC1E 7JE, UK*

Abstract

Floating production, storage, and offloading units (FPSOs) are widely used to develop offshore oil fields from shallow to ultra-deep waters, and some possess fast disconnection systems to avoid harsh environmental conditions. According to a literature survey, the current industry practice is based on the perceptions and experiences of operators to judge the disconnection of these units during cyclonic storms. However, systematic criteria should be established to judge whether disconnection is needed, and the downtime costs and safety issues associated with life-cycle costs should be considered. In this paper, a life-cycle cost model is proposed to optimize (1) the disconnection criteria of FPSOs and (2) the design of their mooring system. Relevant ultimate limit states and reliabilities are considered in association with hull collapse, mooring system failure, and green water impact failure. Effects of downtime costs (deferred production costs), mobilization, and other failure costs are considered. Disconnection criteria are then formulated in terms of the significant wave height and wind speed limits. Because a permanent mooring system may exhibit excessive resistance, it is possible to further optimize the life-cycle cost by reducing the system's resistance until an optimum reliability is obtained, minimizing the costs for non-permanent service. An FPSO in the Gulf of Mexico is selected as an example to illustrate the application of the developed model. The results of this study show that important savings for an overall FPSO project can be achieved by implementing the proposed optimizations.

Keywords: disconnection criteria; FPSO; life-cycle cost; mooring system; target reliability index; ultimate limit state.

Nomenclature

$\cdot$	random variable
$\overline{\Delta}_{ti}$	period of deferred production (yr)
β_{moor}	mooring system reliability index (-)
γ	parameter of mooring system resistance
$\boldsymbol{\Gamma}$	vector of possible values for γ
C_{DPi}	cost of deferred production (USD)
C_{EDi}	cost of environmental damage (USD)
C_F	future cost (USD)

* Corresponding author. Tel.: +82 51 510 2429; fax: +82 51 518 7687.
E-mail address: jeompaik@pusan.ac.kr (JK Paik)

C_{Gi}	general future cost (USD)
C_I	initial cost (USD)
C_{Li}	cost of life loss (USD)
C_{Mi}	cost of mobilization (USD)
C_{Ri}	cost of replacement (USD)
C_T	total life-cycle cost (USD)
C_{Topt}	optimum expected life-cycle cost (USD)
$C_{Topt-moor}$	optimum expected life-cycle cost for an optimized mooring system (USD)
C_{Wi}	cost of injuries or wounds (USD)
d_{ap}	depletion rate at peak production (bbl·yr^{-1})
$E[\cdot]$	expected value
H_L	significant wave height limit (m)
$\mathbf{H_L}$	vector of possible values for significant wave height limit
H_S	significant wave height (m)
j	annual discount rate (yr^{-1})
k	net annual discount rate (yr^{-1})
N	number of broken mooring lines (-)
q_t	annual production rate (bbl·yr^{-1})
$P\{\cdot\}$	probability
P_{fi}	annual probability of failure for the i-th limit state (yr^{-1})
P_{fmoor}	annual probability of failure of mooring system (yr^{-1})
PVF	present value function
R	revenue stream (USD·yr^{-1})
r	inflation rate (yr^{-1})
$\mathcal{R}_i$	resistance for the i-th limit state
$\mathcal{R}_{moor}$	mooring system resistance
$S_{1,sw}$	still-water bending moment (N·m)
$S_{1,wv-hog}$	hogging vertical wave-induced bending moment (N·m)
$S_{1,wv-sag}$	sagging vertical wave-induced bending moment (N·m)
S_i	solicitation for the i-th limit state
T	project life (yr)
t	time (yr)
U	wind speed (m·s^{-1})
U_L	wind speed limit (m·s^{-1})
$\mathbf{U_L}$	vector of possible values for wind speed limit

1. Introduction

1.1. Preliminaries on disconnectable FPSOs

Floating production, storage, and offloading (FPSO) systems are a proven technology for the development of deep offshore oil fields. Their wide area for topside allocation, large storage capacity and adaptability for a wide range of water depths make them a feasible alternative for the production of offshore oil fields from mild to harsh environments.

Some FPSOs with single-point mooring systems (SPMs) can be disconnected to avoid extreme environmental loads, sail toward sheltered areas, and restart operations when the weather becomes benign. The first moored FPSO with a disconnectable turret was introduced in West Australia in 1985, and their use has since been extended to Australia, China, Canada (Mastrangelo et al. 2007), and the Gulf of Mexico (Aanesland et al. 2007; Daniel et al. 2013). Disconnectable mooring systems have several advantages in addition to lowering design loads; they reduce risk to asset damage, make the production of lost infrastructure autonomous, and eliminate the need for helicopter evacuations (Daniel et al. 2013). However, complex mechanisms require disconnection and reconnection, which increases capital expenditure and operational expenditure (Shimamura 2002).

This paper focuses on the disconnection and design criteria for FPSO mooring systems. Several design codes provide requirements for the classification and design of these systems. For example, API (2001) requires floating production systems with fast disconnection systems to withstand the maximum

design conditions when the threshold environment for disconnection is reached. ABS (2014) and LR (2016) define disconnectable units or systems as self-propelled floating units. DNV GL (2017) allows offshore units to be classified as non–self-propelled. Nevertheless, it is outside the scope of these codes to set any disconnection criteria.

Disconnectable SPMs for FPSOs can be classified into those with fast and regular disconnection functions (Li et al. 2014). The former necessitate self-propulsion to achieve quick release and escape from typhoons, cyclones, and hurricanes, and the latter are commonly designed for 100-yr return period conditions. Examples of systems with a regular disconnection function can be seen in the South China Sea, where this alternative has fit well with the construction and operating experience of operators (Li et al. 2014), and in the Mexican Gulf of Mexico, where the mooring system of the FPSO for the KuMaZa field is capable of withstanding hurricane conditions (Aanesland et al. 2007). There are two FPSOs in the US Gulf of Mexico with fast disconnection functions. The FPSO for the Cascade and Chinook fields is self-propelled, and her mooring system is designed to stay connected during 100-yr return period winter storms but to disconnect during hurricanes (Mastrangelo et al. 2007; Daniel et al. 2013). Moreover, her disconnected buoy is designed for 1,000-yr return period loop/eddy currents. Another FPSO in the US Gulf of Mexico, that for the Stones field, also has a fast disconnection function (Leon 2016).

1.2. Previous research on life-cycle cost analysis of marine structures

Life-cycle cost analysis (LCCA) consists of adding the initial costs such as engineering, purchase, fabrication, and installation costs to future costs such as failure, operation, maintenance, and decommissioning costs. Early ideas about its use were proposed by Stahl (1986) for fixed offshore structures and by Bea (1994) for crude-oil carriers. In 1994 and 1997, the International Ship and Offshore Structures Congress (ISSC) adopted the LCCA or so-called economic criteria to evaluate the safety level and risks of ship structures. The total cost of a structure can be expressed as $C_T = C_I + P_F C_F$, where C_I is the initial cost, P_F is the probability of failure over the expected lifetime of the structure, and C_F is the failure cost (Béghin 2010).

Previous applications of LCCA have allowed the optimization of marine structures. For example, the minimization of life-cycle costs has been used to derive reliability indices for the design of fixed offshore structures (Stahl et al. 2000; Kübler & Faber 2004; Campos et al. 2013; Lee et al. 2016) and to establish inspection plans to sustain the reliability index through the service life of these structures (Moan 2011). Maintenance, repair, replacement, and mobilization of equipment costs have been minimized to define a lower deck elevation for fixed offshore platforms (Campos et al. 2015). Bayesian probabilistic network–based consequence models have been used to derive target reliability indices for the design of FPSOs (Faber et al. 2012; Heredia-Zavoni et al. 2012). A multidisciplinary optimization of vessel life-cycle cost with an enhanced multiple-objective collaborative optimizer was developed for the design of naval ships (Temple & Collette 2017).

Marine operations can be also optimized by means of LCCA. The cost of safety improvement for liquefied natural gas transfer arm operations was optimized by means of fuzzy logic with an evidential reasoning algorithm (Nwaoha 2014). Ship oil-drain intervals have been planned by combining oil-analysis program data interpretation and LCCA (Langfitt & Haselbach 2016). With the advent of offshore wind energy, LCCA has been used to optimize vessel chartering strategies for the development of offshore wind farms (Dalgic, Lazakis, Dinwoodie, et al. 2015; Dalgic, Lazakis, Turan, et al. 2015) and to develop tools to evaluate wind farms' life-cycle costs (Lagaros et al. 2015).

1.3. Objectives

The objective of this paper is to derive the target reliability index for the design of the lines in disconnectable mooring systems. To achieve this, a method to define the limit metocean conditions at which an FPSO should be disconnected by a life-cycle cost model is proposed. Then, said model is implemented with expected future costs as a function of failure probability. Minimization of such costs allows to derive an optimum disconnection criterion. Furthermore, a target reliability can be derived by reducing the resistance of the system until the life-cycle cost is optimized.

The current condition for FPSO disconnection is the occurrence of cyclonic storms. Although extensive research has been conducted on the life-cycle cost-based optimization of offshore structures, to our knowledge, no attempt has been made to optimize the disconnection criteria. In this regard, this

paper offers a novel approach to determine the maximum environmental conditions that the mooring system shall withstand as well as the criteria for a reliability-based design.

The remainder of this paper is organized as follows. In Section 2, the mathematical model to calculate the expected life-cycle cost is presented, which allows to determine the limiting environmental conditions for disconnection and define the target reliability index for the mooring system. In Section 3, an applied example of an FPSO in the Gulf of Mexico is used to illustrate the application. In Section 4, results are presented for the calculated disconnection criteria and mooring system target reliability index. Finally, conclusions are given in Section 5.

2. A life-cycle cost model

The present value of the total life-cycle cost C_T of a structure is composed by the initial costs C_I and future costs C_F. Its expected value can be expressed as

$$E[C_T] = E[C_I] + E[C_F] \tag{1}$$

where $E[\cdot]$ denotes the expected value.

The initial cost of a project is well known in comparison with future costs; therefore, $E[C_I] \approx C_I$ is an acceptable approximation. We study the expected future costs due to failure and neglect the failure-independent operational expenditure. Hence, Eq. (1) is rewritten as

$$E[C_T] = C_I + \sum c_i(P_{fi}) \tag{2}$$

where c_i is the expected future cost for the i-th limit state as a function of its annual probability of failure P_{fi}.

2.1. Components of future costs

A holistic approach is used by including economic, social, and environmental effects in the model as advised by De Leon and Ang (2008). Each future cost, also known as failure cost or risk expenditure (RISKEX), can then be written as

$$c_i(P_{fi}) = E[C_{Ri}] + E[C_{Mi}] + E[C_{Wi}] + E[C_{Li}] + E[C_{EDi}] + E[C_{DPi}] \tag{3}$$

where C_{Ri} is the cost of replacement, C_{Mi} is the cost of mobilization, C_{Wi} is the cost of injuries or wounds, C_{Li} is the cost of life loss, C_{EDi} is the cost of environmental damage, and C_{DPi} is the cost of deferred production.

Table 1. Assumptions for calculating failure costs.

Limit state	Definition	Assumptions
ULS hull midship section	The acting vertical bending moment equals or exceeds the hull ultimate strength	The whole FPSO must be replaced with the exception of the subsea systems
ULS mooring system (one line failure)	The acting tension equals or exceeds the breaking load of one mooring line	One mooring line must be replaced
ULS mooring system (two or more line failures)	The acting tension equals or exceeds the breaking load of two or more mooring lines	FPSO drifts off of position, breaking subsea umbilicals and risers
ULS green water at accommodation area	Abnormal wave access to deck in accommodation area	Damage to accommodation area
ULS green water not at accommodation area	Abnormal wave access to deck in process or utility areas	Damage to tanks and processing equipment
Disconnection	FPSO is disconnected to avoid anticipated extreme loads	FPSO is disconnected, mobilized to port under self-propulsion, re-mobilized to site, and reinstalled

Six limit states are included in the model: (I) the ultimate limit state (ULS) of the midship section due to vertical bending moment, (II) the ULS of one mooring line, (III) the simultaneous ULS of two or more mooring lines, (IV) green water at the area of accommodation, (V) green water at other areas, and (VI) FPSO disconnection. The assumptions used to calculate the associated future costs are summarized

in Table 1. A thorough discussion of FPSO limit states is available in an HSE report (Noble Denton Europe Ltd 2001).

Although limit states (II) and (III) could be considered parts of the same limit state, they have different consequences. In fact, mooring systems that comply with API-2SK (API 2005) hold sufficient redundancy to maintain position after one line failure, and therefore the division into two limit states is realistic. Limit state (VI) does not have consequences for life, environment, or infrastructure; however, important economic losses occur when the FPSO is disconnected. Hence, it is desirable to reduce the downtime.

2.2. Expected future costs

The expected value of future costs is derived as in Stahl (1986). A general future cost C_{Gi} at time t is estimated by means of the annual inflation rate r in the form of

$$C_{Gi}\big|_{t=t} = \overline{C_{Gi}} \exp(rt) \tag{4}$$

where $\overline{C_{Gi}}$ is the equivalent cost of failure evaluated at $t = 0$.

By bringing the future costs to the beginning of the project, Eq. (4) becomes

$$C_{Gi}\big|_{t=0} = \overline{C_{Gi}} \exp(rt)\exp(-jt) \tag{5}$$

where j is the annual discount rate.

The expected cost can be estimated as the product of the present value cost and the probability of experiencing that cost. Hence, the expected future cost can be expressed as

$$E[C_{Gi}] = \int_0^T \overline{C_{Gi}}\, P_{fi} \exp(-kt)dt \tag{6}$$

where $k = j - r$ is the net annual discount rate and T is the project life.

The expected future costs in Eq. (3) are readily obtained by solving the integral in Eq. (6), which gives

$$E[C_{Ri}] = \overline{C_{Ri}}\, P_{fi}\, \mathrm{PVF} \tag{7}$$

$$E[C_{Mi}] = \overline{C_{Mi}}\, P_{fi}\, \mathrm{PVF} \tag{8}$$

$$E[C_{Wi}] = \overline{C_{Wi}}\, P_{fi}\, \mathrm{PVF} \tag{9}$$

$$E[C_{Li}] = \overline{C_{Li}}\, P_{fi}\, \mathrm{PVF} \tag{10}$$

$$E[C_{EDi}] = \overline{C_{EDi}}\, P_{fi}\, \mathrm{PVF} \tag{11}$$

where

$$\mathrm{PVF} = [1 - \exp(-kT)]/k \tag{12}$$

is the present value function.

The cost of deferred production necessitates different handling. If the FPSO fails at time t, the deferred production cost under the assumption of replacement after failure equals

$$C_{DPi}(t) = \int_t^T R(\tau)\exp[-k(\tau - t)]d\tau - \int_{t+\Delta t_i}^{T+\Delta t_i} R(\tau)\exp[-k(\tau - t)]d\tau \tag{13}$$

where $R(t)$ is the revenue stream from the product exploitation at t and Δt_i is the period of deferred production while the unit is out of service for the i-th limit state. Substitution of Eq. (13) into (6) gives the expected cost of deferred production

$$E[C_{DPi}] = P_{fi} \int_0^T C_{DPi}(t)\exp(-kt)dt. \tag{14}$$

2.3. Probability of failure

Using the underscore to indicate random variables, the event that the FPSO is connected is defined by the space $\underline{H_S} < H_L \cap \underline{U} < U_L$, where $\underline{H_S}$ is the random significant wave height, H_L is the discrete significant wave height limit for disconnection, $\underline{U}$ is the random wind speed, and U_L is the discrete wind speed limit for disconnection. Noting that the FPSO can only fail in the said space, the probability of failure is written as

$$P_{fi} = P\left\{\underline{S_i} \geq \underline{\mathcal{R}_i} \cap \left(\underline{H_S} < H_L \cap \underline{U} < U_L\right)\right\} \tag{15}$$

where $P\{\cdot\}$ denotes the probability, $\underline{S_i}$ is the solicitation (load or demand), and $\underline{\mathcal{R}_i}$ is the resistance (strength or capacity) for the i-th limit state.

Regarding limit state (I) or the ULS of midship section due to the vertical bending moment, two failure modes are possible: hogging and sagging bending moment failures. By using the appropriate signs, Eq. (15) takes the form of

$$P_{f1} = P\left\{\left(\underline{\mathcal{R}_{1,hog}} - \underline{S_{1,sw}} - \underline{S_{1,wv-hog}} \leq 0\right) \cup \left(\underline{\mathcal{R}_{1,sag}} - \underline{S_{1,sw}} - \underline{S_{1,wv-sag}} \geq 0\right) \cap \left(\underline{H_S} < H_L \cap \underline{U} < U_L\right)\right\} \tag{16}$$

where $\underline{\mathcal{R}_{1,hog}}$ is the hull ultimate strength in the hogging condition, $\underline{S_{1,sw}}$ is the still-water bending moment, $\underline{S_{1,wv-hog}}$ is the hogging vertical wave-induced bending moment, $\underline{\mathcal{R}_{1,sag}}$ is the hull ultimate strength in the sagging condition, and $\underline{S_{1,wv-sag}}$ is the sagging vertical wave-induced bending moment.

For the mooring system, each mooring line is a serial system composed of various sections. The failure of one or more sections of the same line implicates the failure of that mooring line. The probability that one mooring line is broken for limit state (II) is conveniently expressed as

$$P_{f2} = P\left\{\left(\underline{N} = 1\right) \cap \left(\underline{H_S} < H_L \cap \underline{U} < U_L\right)\right\} \tag{17}$$

and the probability that two or more lines are broken for limit state (III) is

$$P_{f3} = P\left\{\left(\underline{N} \geq 2\right) \cap \left(\underline{H_S} < H_L \cap \underline{U} < U_L\right)\right\} \tag{18}$$

where $\underline{N}$ is the number of broken lines.

The probability of green water at the accommodation area can be calculated as

$$P_{f4} = P\left\{\left(\underline{S_4} \leq 0\right) \cap \left(\underline{H_S} < H_L \cap \underline{U} < U_L\right)\right\} \tag{19}$$

for limit state (IV). The probability of green water at other areas in limit state (V) is expressed as

$$P_{f5} = P\left\{\left(\underline{S_5} \leq 0\right) \cap \left(\underline{H_S} < H_L \cap \underline{U} < U_L\right)\right\} \tag{20}$$

where $\underline{S_4}$ and $\underline{S_5}$ represent the vertical relative motion of the deck with respect to the wave surface at the accommodation area and other areas, respectively.

The failure space for limit state (VI) is the complement of the connected FPSO event space. Thus, it is expressed as

$$P_{f6} = P\left\{\underline{H_S} \geq H_L \cup \underline{U} \geq U_L\right\}. \tag{21}$$

2.4. Optimum disconnection criteria

Eq. (15) indicates that the probability of failure is a function of the limit environmental conditions, i.e., $P_{fi} = P_{fi}\left(H_L, U_L\right)$. Let the vectors $\mathbf{H_L}$ and $\mathbf{U_L}$ contain possible values for H_L and U_L, respectively. Accordingly, the optimum expected life-cycle cost can be stated as

$$C_{Topt} = C_I + \min\left[\sum C_i\left(P_{fi}\left(\mathbf{H_L}, \mathbf{U_L}\right)\right)\right] \tag{22}$$

which is associated with an optimum H_L and an optimum U_L.

2.5. Target reliability index for disconnectable mooring systems

Let C_{Topt} be a function of a second function γ that characterizes the mooring system resistance $\mathcal{R}_{moor}$, i.e., $C_{Topt} = C_{Topt}\left(\gamma\left(\mathcal{R}_{moor}\right)\right)$. Therefore, the optimization of C_{Topt} is made possible by solving

$$C_{Topt-moor} = \min\left[C_{Topt}\left(\boldsymbol{\Gamma}\right)\right] \tag{23}$$

where $C_{Topt-moor}$ is the optimum expected life-cycle cost for an optimized mooring system and $\boldsymbol{\Gamma}$ is the vector of possible values for $\gamma\left(\mathcal{R}_{moor}\right)$.

To determine Eq. (23), some variables must be expressed as functions of the mooring system resistance. For this model, $C_I = C_I\left(\gamma\left(\mathcal{R}_{moor}\right)\right)$, $C_{R2} = C_{R2}\left(\gamma\left(\mathcal{R}_{moor}\right)\right)$, $C_{M2} = C_{M2}\left(\gamma\left(\mathcal{R}_{moor}\right)\right)$, $C_{R3} = C_{R3}\left(\gamma\left(\mathcal{R}_{moor}\right)\right)$, $C_{M3} = C_{M3}\left(\gamma\left(\mathcal{R}_{moor}\right)\right)$, $P_{f2} = P_{f2}\left(\gamma\left(\mathcal{R}_{moor}\right)\right)$, and $P_{f3} = P_{f3}\left(\gamma\left(\mathcal{R}_{moor}\right)\right)$. Possible candidates for $\gamma\left(\mathcal{R}_{moor}\right)$ are the mooring line thickness, weight, line strength, and overall mooring system strength. In Section 4.2, this function is taken as the minimum breaking load (MBL) of the top mooring line section.

Because limit states (II) and (III) exclude each other, the probability of failure of the mooring system P_{fmoor} is simply calculated as

$$P_{fmoor} = P_{f2} + P_{f3} \tag{24}$$

from which the mooring system reliability index β_{moor} can be calculated. The latter is defined as

$$\beta_{moor} = -\Phi^{-1}\left(P_{fmoor}\right) \tag{25}$$

where $\Phi^{-1}\left(\cdot\right)$ is the inverse standard normal cumulative distribution function.

The target β_{moor} is the one associated with $C_{Topt-moor}$ in Eq. (23) because this value minimizes the life-cycle cost for a disconnectable FPSO.

2.6. Life-cycle cost-based optimization

The proposed life-cycle cost model is implemented in a Matlab routine. Its algorithm is described by Fig. 1. The first step is to carry out Monte Carlo simulation to sample the random resistances of the different limit states and the random input variables for the solicitations.

Kriging metamodels are then used to estimate different solicitations on the FPSO with the ooDACE Matlab toolbox (Couckuyt et al. 2010; Couckuyt et al. 2012; Ulaganathan et al. 2015). Metamodels are approximate functions that serve to predict the responses of several input parameters. They require design of computer experiments techniques such as Latin hypercube sampling (LHS) to establish credible scenarios and feed the metamodels. A background on metamodel methods can be found in Fang et al. (2006), and detailed information about their application in marine structures is documented in the literature (Yang & Zheng 2011; Garrè & Rizzuto 2012; Cabrera-Miranda & Paik 2017).

The LCCA is conducted inside the disconnection criteria optimization loop, which is in turn embedded into the mooring system optimization loop. Another Monte Carlo simulation is built in the major loop to study the influence of the mooring system resistance. Finally, the optimum life-cycle costs with associated disconnection criteria and mooring system reliability index are obtained as outputs.

This approach assumes that the load remains unchanged after the mooring system's resistance is reduced. This is a conservative assumption, because a weak mooring system has less stiffness and consequently a less static component of tension than a robust one.

3. Applied example

In this section, an example is used to illustrate the application of the proposed life-cycle cost model. First, the floater characteristics are presented. To carry out the reliability analysis and determine the failure probabilities, solicitations are investigated by means of a metamodel approach. Probabilistic distributions for resistances are taken from the literature. Finally, the probabilities of failure are used to estimate the expected value of the life-cycle cost.

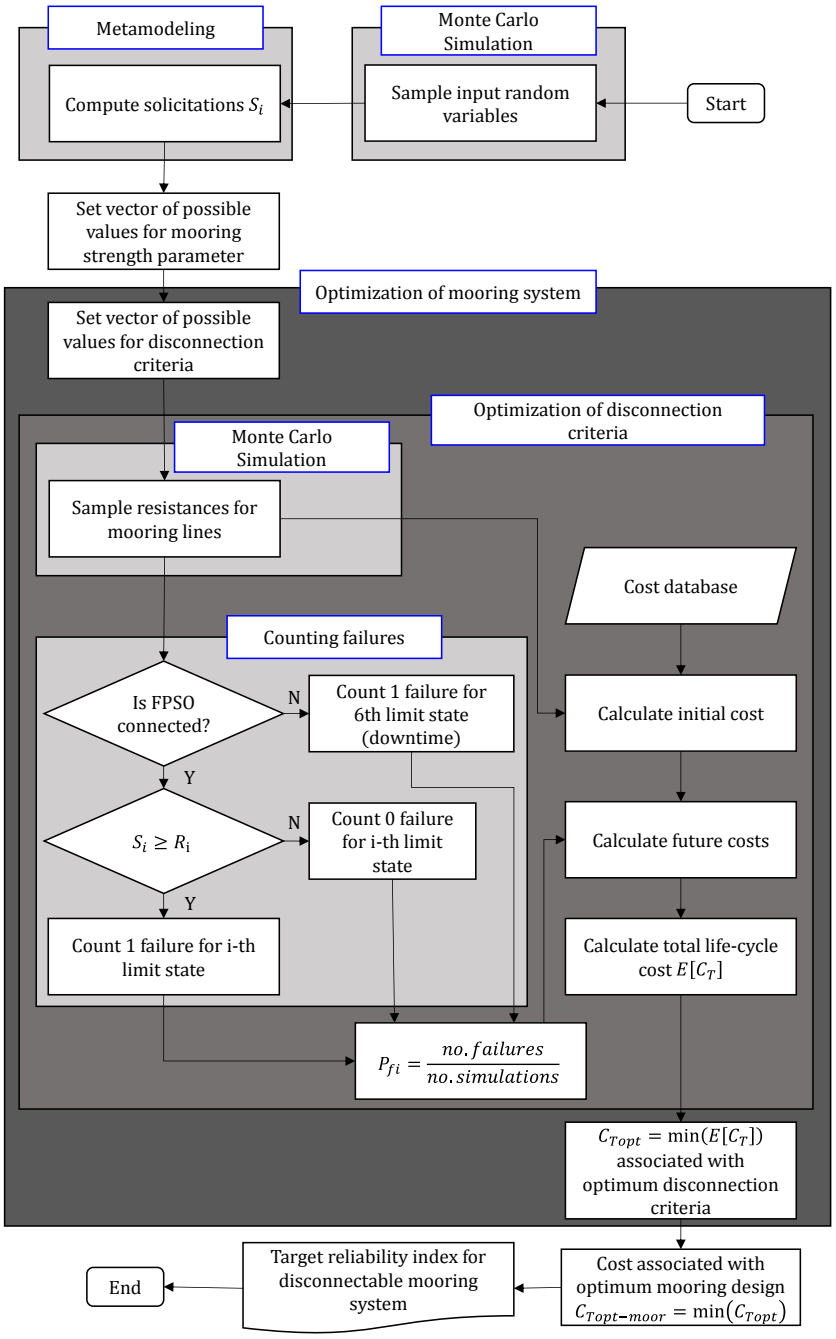

Figure. 1. Data flow chart for the design optimization of an FPSO's disconnectable mooring systemn.

3.1. FPSO characteristics

Let a hypothetical tanker-based FPSO be considered for service as the host of an offshore oil field in the Mexican Gulf of Mexico in a 3,100-m water depth over 15-yr. Her mooring system is of the SPM buoy turret mooring type with a fast disconnection function. She also possesses self-propulsion. Her dimensions are presented in Table 2.

The mooring system consists of three clusters of three taut legs each, for a total of 12 lines. Each line is composed of a 114.3-mm diameter grade 4 chain bottom section 150-m in length; a 190.5-mm diameter polyester section 3,704-m in length; and a 114.3-mm diameter grade 4 chain top section 150-m in length. The system was designed according to industry-accepted guidelines (API 2005; DNV GL 2015) for sea states with 100-yr return period waves, 100-yr return period wind, and 10-yr return period current.

Table 2. Main particulars of a hypothetical tanker-shaped FPSO.

Particular	Dimension
Length between perpendiculars	239-m
Breadth	42-m
Depth	21-m
Dead weight	108,000-t
Total cargo capacity	107,000-m^3 (680,000-bbl)

3.2. Solicitation metamodels

The LHS technique was applied to select 50 scenarios and investigate the solicitations as a function of the environmental and functional conditions (see Table 3). The wave parameters were taken from DNV (2014), and the wind and current distributions were derived from data in API (2007). The directions of the environment were approximated by means of directional functions, and the vessel's draft was assumed to follow a uniform distribution.

Table 3. Probabilistic distribution of input variables for the solicitation metamodels.

Variable	Unit	Distribution
Significant wave height	m	Weibull (α =1.81, β =1.47)
Zero-crossing wave period	s	Lognormal distribution ($\mu = 0.7 + 0.95 H_S^{0.158}$, $\sigma = 0.07 + 0.1685 \exp[-0.0312 H_S]$)
Wave direction angle with respect to peak direction	rad	Directional function (s =5)
1-h average wind speed at 10 m above sea level	$m \cdot s^{-1}$	Log-normal (μ =0.61, σ =0.725)
Wind direction angle respect to peak direction	rad	Directional function (s =5)
Current speed at surface	$m \cdot s^{-1}$	Log-normal (μ =−1.1187, σ =0.432)
Current direction angle respect to peak direction	rad	Directional function (s =5)
Draft	m	Uniform (6.38,15.85)

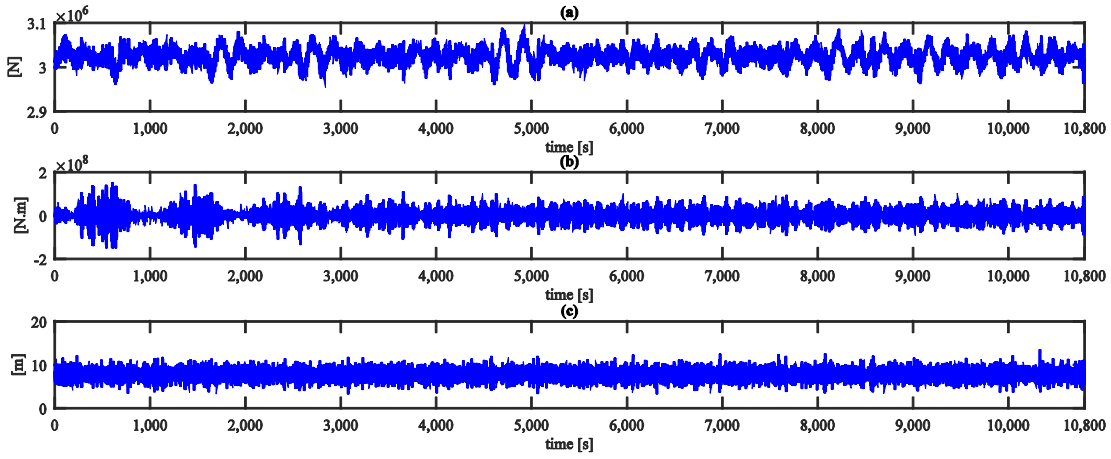

Figure. 2. Time-domain series of FPSO responses of a typical scenario for (a) mooring line tension at the top chain section for the most loaded line, (b) vertical wave-induced bending moment, and (c) deck vertical motion relative to the wave surface at the bow.

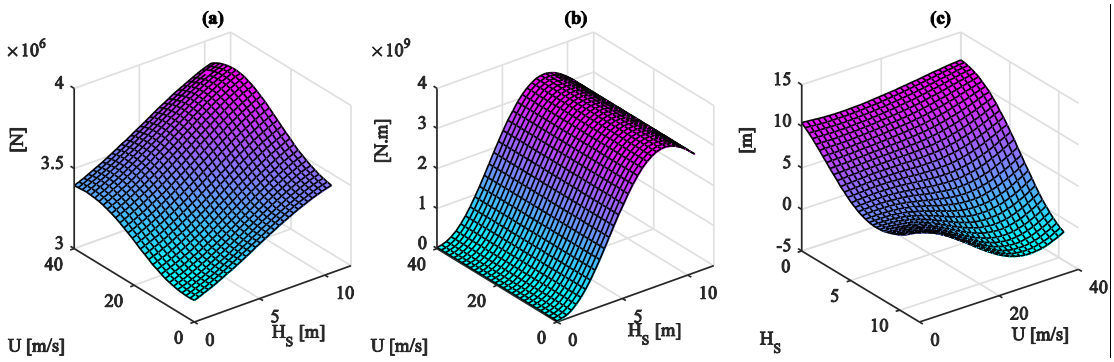

Figure 3. Predicted solicitations by Kriging metamodels (variables not shown are set to their mean value) for (a) mooring line tension at the top chain section of the most loaded line, (b) hogging vertical wave-induced bending moment, and (c) deck vertical motion relative to the wave surface at the bow.

For each scenario, station-keeping analyses were conducted with ANSYS Aqwa in the time domain. The irregular waves were defined by the Pierson-Moskowitz spectrum, the wind by the ISO spectrum, and the current by a slab profile. Time series of responses, like those shown in Fig. 2, were obtained and analyzed. For each scenario, we extracted the maximum mooring line tension; the maximum and minimum vertical wave-induced bending moment for hogging and sagging, respectively; and the minimum vertical relative motion at four locations at the deck.

The input variables and responses for each scenario were then used to build the metamodels. A few of the predicted solicitations are plotted in Fig. 3. Overall, 42 metamodels were computed that consisted of 36 tensions for mooring line sections, two vertical wave-induced bending moments for hogging and sagging, and four vertical motions relative to the wave surface at the bow, aft, port, and starboard. Initially, the metamodels were inaccurate for extreme loads, and therefore 10 additional scenarios were uniformly sampled between the maximum values of the LHS and the 100-yr return period conditions to improve the predictions of the metamodels. Furthermore, wind speed and its direction and current speed and its direction were excluded from the models for bending moments to reduce the mean error. The remaining solicitations were modeled as functions of the eight variables (see Table 3).

3.3. Reliability analysis

Reliability analysis aims to calculate the failure probability for a certain limit state. In addition to the random solicitations predicted by metamodels, other random variables had to be considered. The still-water bending moment in Table 4 is described via a bimodal distribution as proposed by Ivanov et al. (2011). This consists of two truncated normal distributions that describe hogging and sagging as two sides of one phenomenon. Huang and Moan (2005) demonstrated that FPSOs were sometimes operated under still-water loads above the rule moment. Therefore, we used 1.3 times the design still-water bending moment, as indicated in the Common Structural Rules (IACS 2012). Moments minima were taken as 6% of the design moments. Furthermore, we used a coefficient of variation of 0.6 for both hogging and sagging, which fell within the range of values in the second paper.

Table 4. Random variables for the reliability analysis.

Description	Unit	Distribution
Still-water bending moment	N.m	Bimodal from truncated normal for sagging (μ =−1.347×109, σ =8.08×108, b_l =−2.57×109, b_u =−1.19×108, K_s =0.6) and truncated normal for hogging (μ =1.735×109, σ =1.04×109, b_l =1.53×108, b_u =3.31×109, K_h =0.4)
Ultimate hull girder strength in hogging	N.m	Log-normal (μ =22.99, σ =0.09975)
Ultimate hull girder strength in sagging	N.m	Log-normal (μ =22.797, σ =0.09975)
Ultimate strength for chain	N	Log-normal (μ =16.2826, σ =0.0499)
Ultimate strength for polyester rope	N	Log-normal (μ =16.1148, σ =0.0499)

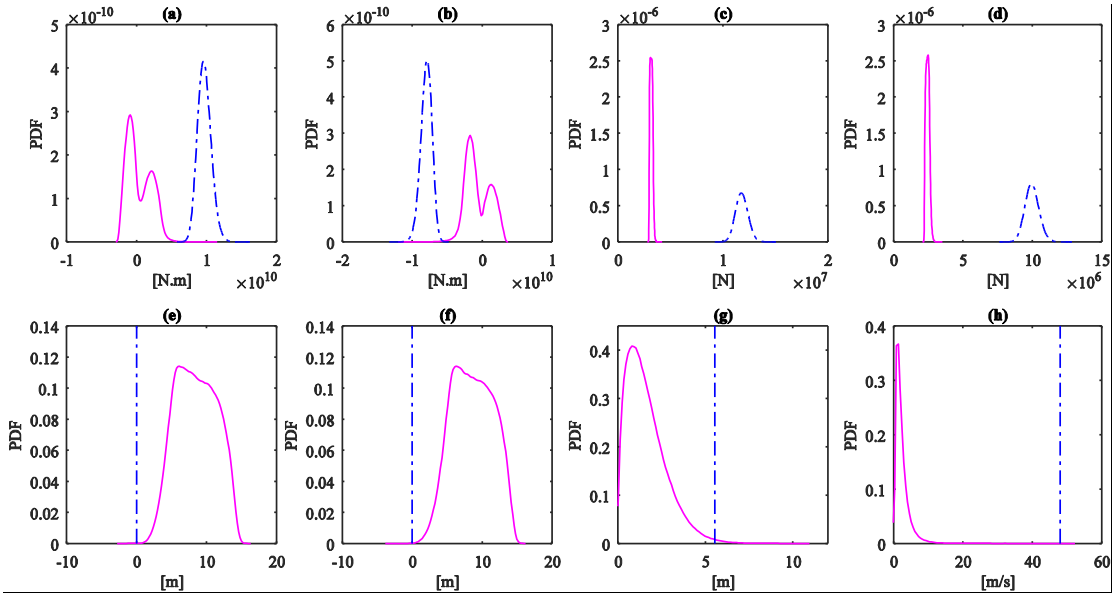

Figure 4. PDF of resistances (dot-dashed line) and solicitations (continuous line) for FPSO limit states without disconnection: (a) hogging bending moment, (b) sagging bending moment, (c) tension at top-chain section of most loaded line, (d) tension at intermediate polyester section of most loaded line, (e) green water at accommodation, (f) green water at bow, (g) significant wave height and optimum disconnection limit, (h) wind speed and optimum disconnection criterion.

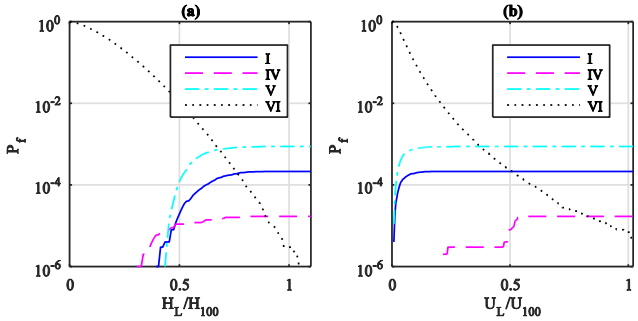

Figure 5. Probabilities of failure as function of (a) significant wave height limit and (b) wind speed limit.

Resistances for hull and mooring lines are usually assumed to follow a log-normal distribution. Their parameters for this study are indicated in Table 4. The mean of the former was taken as the ultimate strength of a tanker of similar dimensions with half corrosion addition in Kim et al. (2014). The coefficient of variation was taken as 0.1, as suggested by Sun and Bai (2001). The parameters for the resistance of mooring lines were taken from Vazquez-Hernandez et al. (2006).

The reliability analysis was carried out using the Monte Carlo simulation method with 1×10^6 simulations for a total of 47 random variables, some of which were used to estimate solicitations. Fig. 4 displays a comparison of the probability density functions (PDFs) for solicitations and resistances. Afterward, limit state violations were evaluated, and the failure probabilities were then estimated. In Fig. 5, the later ones are calculated as functions of an arbitrary single disconnection criterion, where H_L and U_L are normalized with respect to the 100-yr return period significant wave height H_{100} and 100-yr return period 1-hour average wind speed U_{100}, respectively. They in turn correspond to 10.13 m and 48 m/s, respectively.

No failure scenarios were found for limit states (II) and (III); thus, we conclude that $P_{f2} < 1 \times 10^{-6}$ and $P_{f3} < 1 \times 10^{-6}$. This can be better understood by examining the wide safety margin between solicitations and resistances in Fig. 4(c) and (d).

3.4. Life-cycle cost analysis

Initial and future costs for replacement and reposition were calculated by means of QUE$TOR, a capital expenditure/operational expenditure cost estimation software for oil and gas projects (IHS Markit 2017). Wounds, life loss, and environmental damage costs were estimated based on local regulations. Table 5 summarizes the equivalent costs of failure in normalized fashion with respect to the initial cost of the project. The net annual discount rate was taken as 12% for the economical evaluation.

Production costs were also calculated with QUE$TOR, which were deducted from the oil sales along with royalties and taxes. The expected production profile was replaced by an approximate profile to ease the estimation of the deferred production cost as depicted in Fig. 6, where the annual production rate q_t is normalized with respect to the depletion rate at peak production d_{ap}. The approximate profile satisfies the conditions of keeping the ultimately recoverable resources at the end of the project and holding the peak of the plateau in magnitude and time.

Table 5. Equivalent cost of failure at $t = 0$.

Limit state	$\overline{C_R}/C_I$	$\overline{C_M}/C_I$	$\overline{C_W}/C_I$	$\overline{C_L}/C_I$	$\overline{C_{ED}}/C_I$	$E[C_{ue}]/(C_I P_f \text{ PVF})$
ULS hull midship section	0.8937	0.0006	0.0000	0.0060	0.0119	0.1892
ULS mooring system (one line failure)	0.0021	0.0011	0.0000	0.0000	0.0000	0.0007
ULS mooring system (two or more lines failure)	0.1063	0.0006	0.0023	0.0023	0.0091	0.1285
ULS green water at accommodation area	0.0025	0.0004	0.0012	0.0012	0.0047	0.0011
ULS green water not at accommodation area	0.0079	0.0004	0.0009	0.0009	0.0034	0.0011
Disconnection	0.0000	0.0127	0.0000	0.0000	0.0000	0.0011

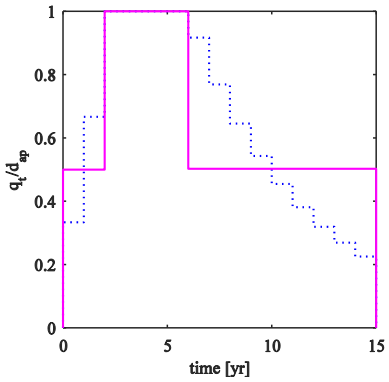

Figure 6. Actual (dotted line) and approximate (solid line) hydrocarbon liquid production profile to calculate costs of deferred production.

4. Computed Results and Discussions

In this section, the calculated optimum disconnection criteria of the applied example are presented. A target reliability index for the mooring system is later derived by reducing its resistance until the life-cycle cost is optimized.

4.1. Calculated optimum disconnection criteria

Life-cycle costs were evaluated as a function of the disconnection criteria. A screening analysis was conducted for $0 \le H_L/H_{100} \le 1.1$ and $0 \le U_L/U_{100} \le 1.1$, and a definitive analysis was conducted for $0.44 \le H_L/H_{100} \le 1.03$ and $0.2 \le U_L/U_{100} \le 1$ in a mesh of 30×30 points. The latter results are plotted in Fig. 7(a). The optimum disconnection criteria were found. The associated variables are summarized in the second row of Table 6, where C_{I_0} is the initial cost of the FPSO with the rule-based designed mooring system.

In Fig. 8, the exceedance curves demonstrate that most of the solicitations are reduced after the optimum disconnection criteria are implemented. Exceptions include the relative vertical motions for green water limit states (IV) and (V) in Fig. 8(e) and (f), respectively, where disconnection has little influence.

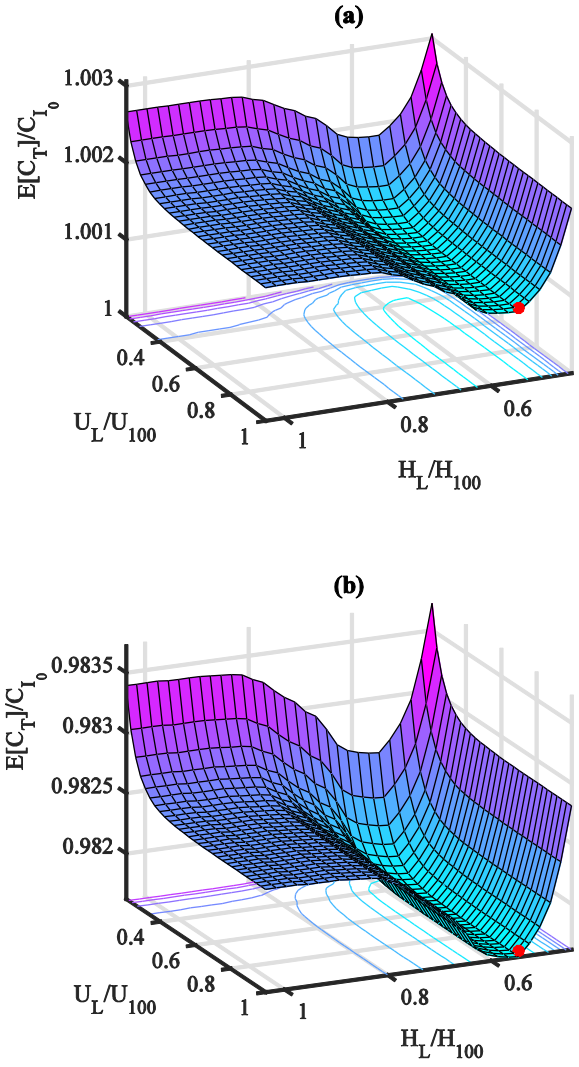

Figure 7. Expected life-cycle cost for FPSO with (a) a rule-based designed mooring system and (b) an optimized mooring system (optimum is shown as red point).

Table 6. Calculated optimum disconnection criteria and mooring system reliability index.

Case	H_L	U_L	P_{f6} (downtime per yr)	$E[C_T]/C_{I_0}$ without disconnection	C_{Topt}/C_{I_0}	β_{moor} with optimum disconnection
FPSO with rule-based designed mooring system	5.5345 m	48 m/s	0.0057	1.0017	1.0009	>4.7534
FPSO with optimized disconnectable mooring system	5.5345 m	48 m/s	0.0057	0.9822	0.9816	2.156 (target)

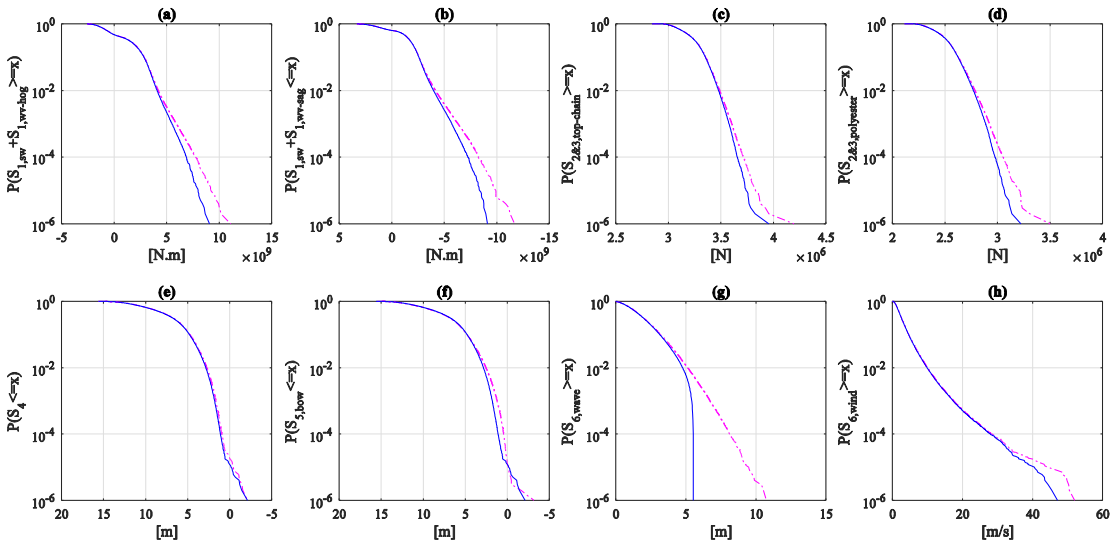

Figure 8. Exceedance curves for solicitations when no disconnection (dash-dotted line) is anticipated and with optimum disconnection (solid line).

4.2. Calculated target reliability index for mooring system

The optimum expected life-cycle costs were calculated as a function of the mooring line MBL by assuming that all of the sections had the same MBL but different material, diameter, and associated costs. First, we calculated the initial, replacement, and mobilization costs of the mooring system, as illustrated in Fig. 9. We then performed Monte Carlo simulation to obtain the resistance distribution for each mooring line section. Afterwards, the optimum life-cycle cost was calculated as in Section 4.1. The procedure was repeated for each analyzed MBL. The results are plotted in Fig. 10.

The expected life-cycle cost for the optimized mooring system design is plotted in the vicinity of its optimum in Fig. 7(b). The probability of failure at this point is $P_{fmoor} = 1.55 \times 10^{-2}$, and the associated parameters are presented in the last row of Table 6. The calculated target reliability index is 2.156, which is recommended to be raised to 2.3 in order to comply with suggested values for the ultimate limit state design of structures with relative high effort to achieve reliability and insignificant expected failure consequences (Rackwitz 2000).

In Fig. 11, it becomes evident that the rule-based design has a resistance surplus and that the economic analysis has determined an optimum safety margin. Fig. 12 illustrates that the probability of failure for the mooring system is dominated by the failure of one line rather than by the failure of two or more lines; therefore, the consequences are not that onerous (see Table 5).

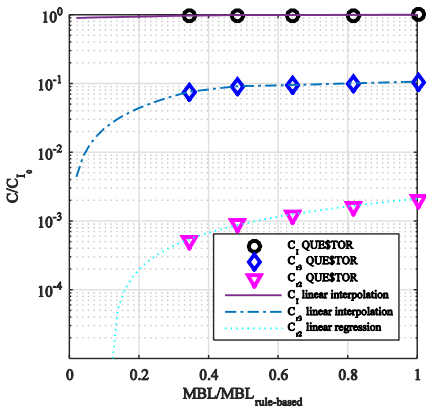

Figure 9. Initial and future costs at present time in association with mooring line resistance.

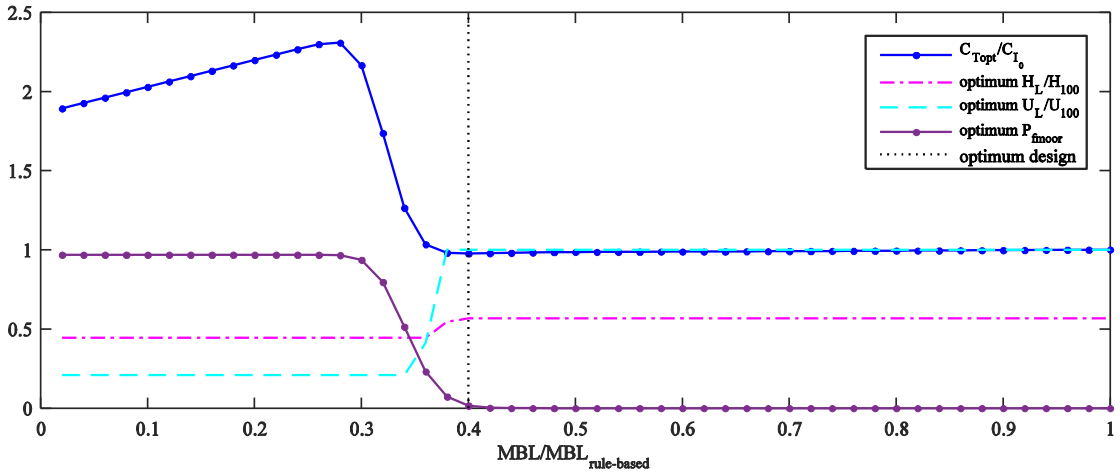

Figure 10. Optimum life-cycle cost and associated variables in association with mooring line resistance.

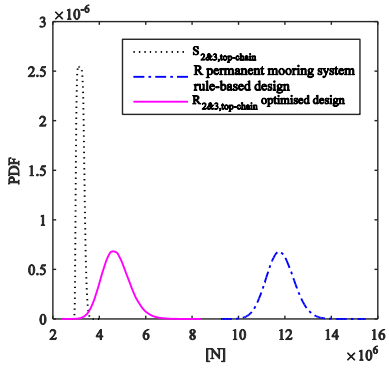

Figure 11. Comparison of PDF for solicitation and resistance for rule-based designed mooring system and optimized mooring system.

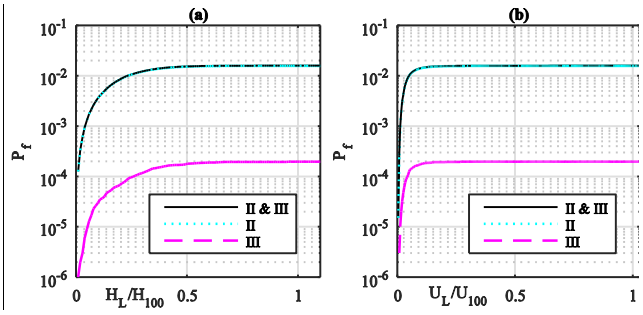

Figure 12. Probabilities of failure for optimum mooring system as a function of (a) significant wave height limit and (b) wind speed limit.

5. Conclusions

The industry practice on disconnectable FPSOs consists of disconnecting said units when cyclonic storms approach and designing mooring systems for 100-yr return period non-cyclonic storms according to API-RP-2SK. However, it is highly desirable to establish a systematic procedure to derive disconnection and design criteria based on a cost-effective decision.

The objective of the present study has been to derive a target reliability index for the design of mooring lines of disconnectable FPSOs. Said goal has been fulfilled by means of a proposed life-cycle cost model which can be used to optimize the disconnection criteria for FPSOs and subsequently to obtain a design criteria under reliability format.

A hypothetical tanker shaped FPSO was used to illustrate the application of the model. The calculated target reliability index for the disconnectable mooring system is 2.156 and the limit significant wave height is 5.35 m. Wind speed was found not to be a dominant parameter for the minimization of failure costs for this problem.

Main contributions of this research are: (1) the provision of a life-cycle model for disconnectable FPSO projects that serves as a framework for optimization of the disconnection and design criteria of mooring systems (2) as well as an algorithm for its implementation. Moreover, the results of the applied example show that savings of up to 2.01% of the initial cost of the project can be achieved if the optimization of the mooring system design is carried out (see Table 6). Although these features cannot be generalized, we expect other FPSO projects to cut production costs if the proposed optimizations are used.

There is one important limitation in the implementation of the optimum disconnection criteria. Although cyclonic-storms can be well predicted in advance, extra-tropical storms tend to develop quickly, and therefore it is difficult or impossible to initiate a planned disconnection. Thus, the distinction between the two types of said storms would offer an appreciable improvement for the current life-cycle cost model and algorithm.

Acknowledgements

This study was undertaken at the Korea Ship and Offshore Research Institute at Pusan National University which has been a Lloyd's Register Foundation (LRF) Research Centre of Excellence since 2008. The authors are grateful to Dr. Alberto Omar Vazquez-Hernandez of the Mexican Petroleum Institute (IMP) for his valuable discussion on the design of mooring systems. The first author would like to acknowledge the scholarship from the Mexican National Council for Science and Technology (CONACYT). The second author wishes to thank the financial support of PRH-15 ANP program.

References

Aanesland V, Kaalstad JP, Bech A, Holm A, Production NF. 2007. Disconnectable FPSO—Technology To Reduce Risk in GoM. In: Offshore Technol Conf. Houston, USA; p. OTC 18487.

[ABS] American Bureau of Shipping. 2014. Rules for building and classing Floating Production Instalations. Houston, USA.

[API] American Petroleum Institute. 2001. Recommended Practice for Planning, Designing, and Constructing Floating Production Systems, *API Recommended Practice 2FPS*. First. Washington, D.C.

[API] American Petroleum Institute. 2005. Design and Analysis of Stationkeeping Systems for Floating Structures *Recommended Practice 2SK*. Third. Washington, D.C.

[API] American Petroleum Institute. 2007. Interim Guidance on Hurrican Conditions in the Gulf of Mexico *API Bulletin 2INT-MET*. Washington, D.C.

Bea RG. 1994. Evaluation of Alternative Marine Structural Integrity Programs. *Mar Struct*. 7:77–90.

Béghin D. 2010. Reliability-Based Structural Design. In: Hughes OF, Paik JK, editors. Sh Struct Anal Des. Jersey City, New Jersey: The Society of Naval Architects and Marine Engineers; p. 5-1-5–63.

Cabrera-Miranda JM, Paik JK. 2017. On the probabilistic distribution of loads on a marine riser. *Ocean Eng*. 134:105–118.

Campos D, Cabrera Miranda JM, Martínez Mayorga JM, García Tenorio M. 2013. Optimal Metocean Design of Offshore Tower Structures. In: Proc ASME 2013 32nd Int Conf Ocean Offshore Arct Eng OMAE2013. Nantes, France: ASME; p. OMAE2013-10953.

Campos D, Ortega C, Alamilla JL, Soriano A. 2015. Selection of Design Lower Deck Elevation of Fixed Offshore Platforms for Mexican Code. *J Offshore Mech Arct Eng*. 137:51301-1-51301–8.

Couckuyt I, Declercq F, Dhaene T, Rogier H, Knockaert L. 2010. Surrogate-Based Infill Optimization

Applied to Electromagnetic Problems. *Int J RF Microw Comput Eng*. 20:492–501.

Couckuyt I, Forrester A, Gorissen D, De Turck F, Dhaene T. 2012. Blind Kriging: Implementation and performance analysis. *Adv Eng Softw*. 49:1–13.

Dalgic Y, Lazakis I, Dinwoodie I, McMillan D, Revie M, Majumder J. 2015. Cost benefit analysis of mothership concept and investigation of optimum chartering strategy for offshore wind farms. *Energy Procedia*. 80:63–71.

Dalgic Y, Lazakis I, Turan O, Judah S. 2015. Investigation of optimum jack-up vessel chartering strategy for offshore wind farm O & M activities. *Ocean Eng*. 95:106–115.

Daniel J, Mastrangelo CF, Ganguly P. 2013. First Floating , Production Storage and Offloading vessel in the U.S. Gulf of Mexico. In: Offshore Technol Conf. Houston, USA; OTC 24112.

[DNV] Det Norske Veritas AS. 2014. *Recommended practice DNV-RP-C205*, Environmental Conditions and Environmental Loads. [place unknown].

DNV GL. 2015. *Offshore Standard DNVGL-OS-E301*, Position mooring. [place unknown].

DNV GL. 2017. *Rules for Classification, Offshore units, DNVGL-RU-OU-0102* Floating production, storage and loading units. [place unknown].

Faber MH, Straub D, Heredia-Zavoni E, Montes-Iturrizaga R. 2012. Risk assessment for structural design criteria of FPSO systems. Part I: Generic models and acceptance criteria. *Mar Struct*. 28:120–133.

Fang K, Li RZ, Sudjianto A. 2006. Design and modeling for computer experiments. Boca Raton, FL, USA: Chapman & Hall/CRC.

Garrè L, Rizzuto E. 2012. Bayesian networks for probabilistic modelling of still water bending moment for side-damaged tankers. *Ships Offshore Struct*. 7:269–283.

Heredia-Zavoni E, Montes-Iturrizaga R, Faber MH, Straub D. 2012. Risk assessment for structural design criteria of FPSO systems. Part II: Consequence models and applications to determination of target reliabilities. *Mar Struct*. 28:50–66.

Huang W, Moan T. 2005. Combination of global still-water and wave load effects for reliability-based design of floating production, storage and offloading (FPSO) vessels. *Appl Ocean Res*. 27:127–141.

IHS Markit. 2017. QUE$TOR (https://www.ihs.com/products/questor-oil-gas-project-cost-estimation-software.html).

[IACS] International Association of Classification Societies. 2012. Common Structural Rules for Oil Tankers. [place unknown].

Ivanov LD, Ku A, Huang B-Q, Krzonkala VCS. 2011. Probabilistic presentation of the total bending moments of FPSOs. *Ships Offshore Struct*. 6:45–58.

Kim DK, Kim HB, Zhang X, Li CG, Paik JK. 2014. Ultimate strength performance of tankers associated with industry corrosion addition practices. *Int J Nav Archit Ocean Eng*. 6:507–528.

Kübler O, Faber MH. 2004. Optimality and Acceptance Criteria in Offshore Design. *J Offshore Mech Arct Eng*. 126:258–264.

Lagaros ND, Karlaftis MG, Paida MK. 2015. Stochastic life-cycle cost analysis of wind parks. *Reliab Eng Syst Saf*. 144:117–127.

Langfitt Q, Haselbach L. 2016. Coupled oil analysis trending and life-cycle cost analysis for vessel oil-change interval decisions interval decisions. *J Mar Eng Technol*. 15:1–8.

Lee S, Jo C, Bergan P, Pettersen B, Chang D. 2016. Life-cycle cost-based design procedure to determine the optimal environmental design load and target reliability in offshore installations.

Struct Saf. 59:96–107.

Leon A. 2016. Breaking new frontiers. *Offshore Eng* Sept.:22–25.

De Leon D, Ang AHS. 2008. Confidence bounds on structural reliability estimations for offshore platforms. *J Mar Sci Technol*. 13:308–315.

Li D, Yi C, Xu Z, Bai X. 2014. Scenario Research and Design of FPSO in South China. In: Proc Twenty-fourth Int Ocean Polar Eng Conf. Vol. ISOPE-I-14. Busan, Korea: International Society of Offshore and Polar Engineers (ISOPE); p. 964–969.

[LR] Lloyd's Register. 2016. Rules and Regulations for the Classification of Offshore Units. London: Lloyd's Register Group Limited.

Mastrangelo C, Barwick K, Fernandes L, Theisinger E. 2007. FPSOs in the Gulf of Mexico [presentation material]. In: Inf Transf Meet. Kenner, Louisiana, USA.

Moan T. 2011. Life-cycle assessment of marine civil engineering structures. *Struct Infrastruct Eng*. 7:11–32.

Noble Denton Europe Ltd. 2001. Rationalisation of FPSO design issues—Relative reliability levels achieved between different FPSO limit states. Norwich: Health & Safety Executive.

Nwaoha TC. 2014. Inclusion of hybrid algorithm in optimal operations of liquefied natural gas transfer arm under uncertainty. *Ships Offshore Struct*. 9:514–524.

Rackwitz R. 2000. Optimization — the basis of code-making and reliability verification. *Struct Saf*. 22:27–60.

Shimamura Y. 2002. FPSO/FSO : State of the art. *J Mar Sci Technol*. 7:59–70.

Stahl B. 1986. Reliability Engineering and Risk Analysis. In: McClelland B, Reifel MD, editors. Plan Des fixed offshore platforms. New York: Van Nostrand Reinhold Company; p. 59–98.

Stahl B, Aune S, Gebara JM, Cornell CA. 2000. Acceptance Criteria for Offshore Platforms. *J Offshore Mech Arct Eng*. 122:153.

Sun H-H, Bai Y. 2001. Time-Variant Reliability of FPSO Hulls. *SNAME Trans*. 109:341–366.

Temple D, Collette M. 2017. Understanding lifecycle cost trade-offs for naval vessels: minimising production, maintenance, and resistance. *Ships Offshore Struct*. 12:756–766.

Ulaganathan S, Couckuyt I, Deschrijver D, Laermans E, Dhaene T. 2015. A Matlab toolbox for Kriging metamodelling. *Procedia Comput Sci*. 51:2708–2713.

Vazquez-Hernandez AO, Ellwanger GB, Sagrilo LVS. 2006. Reliability-based comparative study for mooring lines design criteria. *Appl Ocean Res*. 28:398–406.

Yang HZ, Zheng W. 2011. Metamodel approach for reliability-based design optimization of a steel catenary riser. *J Mar Sci Technol*. 16:202–213.